

# Materials Advances

[rsc.li/materials-advances](https://rsc.li/materials-advances)



ISSN 2633-5409

**PAPER**

Haruyasu Asahara, Hiroshi Uyama *et al.*  
Surface modification of polylactic acid using a photo-activated  
chlorine dioxide process: surface properties and dissimilar  
adhesion

Cite this: *Mater. Adv.*, 2025,  
6, 1608

# Surface modification of polylactic acid using a photo-activated chlorine dioxide process: surface properties and dissimilar adhesion†

Haruyasu Asahara,<sup>a</sup> Weiting Wu,<sup>c</sup> Taka-Aki Asoh,<sup>‡</sup> Yu-I Hsu,<sup>‡</sup>  
Tsuyoshi Inoue<sup>ab</sup> and Hiroshi Uyama<sup>ib</sup>\*Received 23rd December 2024,  
Accepted 10th February 2025

DOI: 10.1039/d4ma01275e

rsc.li/materials-advances

In this study, we examined the modification of polylactic acid (PLA) plates and powders using a photo-activated chlorine dioxide ( $\text{ClO}_2^*$ ) treatment. Changes in the degree of oxidation depending on the oxidation conditions, namely, temperature and time, were determined by surface elemental analysis using X-ray photoelectron spectroscopy and quantification of the number of carboxy groups using toluidine blue O staining. Oxidized PLA exhibited excellent adhesion to dissimilar materials, including aluminum and cellulose. In the adhesion to aluminum, the relationship between the adhesion strength and oxidation degree was investigated.

## 1. Introduction

Poly(lactic acid) (PLA) is a biodegradable polymer produced from renewable resources and is attracting attention as an environmentally friendly material.<sup>1–3</sup> As the plastic waste problem has become more serious in recent years, the demand for biodegradable polymers such as PLA has been rapidly increasing. Owing to its excellent physical properties and biodegradability, PLA finds application in a variety of fields, including packaging materials,<sup>4–6</sup> medical devices,<sup>7</sup> textiles,<sup>8,9</sup> and agricultural films.<sup>10,11</sup> In addition, the versatile properties of PLA are suitable for fused deposition modelling (FDM) 3D printers, and it is widely used for both household and industrial applications.<sup>12–16</sup> However, PLA has several limitations, of which low adhesion to dissimilar materials is one of the most notable. The low adhesive property of PLA is attributed to its low surface energy and the chemical and physical properties of its surface. Various approaches have been proposed to adhere PLA to different materials, of which surface modification is one of the most popular and important.<sup>17</sup> Surface modification,<sup>18,19</sup> including physical modification (*e.g.*, plasma treatment<sup>20–24</sup> and UV irradiation<sup>25,26</sup>) and chemical modification (*e.g.*, alkaline treatment<sup>27,28</sup> and photografting<sup>29,30</sup>), can alter the material surface

properties without affecting the bulk properties. Although these methods can improve adhesion by introducing polar functional groups onto the surface of PLA, their poor reproducibility and the complexity of the treatment process have led to a demand for the development of a new method. In addition, existing methods are not suitable for processing moldings created by 3D printers. Therefore, a new method that can be applied to complex moldings while maintaining their strength is desirable.

We reported that photo-activated chlorine dioxide radical ( $\text{ClO}_2^*$ ) gas acts as an efficient oxidizing agent in C–H bond oxygenation reactions and can be applied for oxidative surface modification of various polymers, such as polypropylene (PP),<sup>31–34</sup> acrylonitrile butadiene styrene,<sup>35</sup> polycarbonate,<sup>36</sup> polyhydroxyalkanoate,<sup>37</sup> and poly(phenylene sulfide).<sup>38</sup> Additionally, it has already been demonstrated that carboxy groups are introduced to the PLA surface by applying photo-activated  $\text{ClO}_2^*$  gas treatment.<sup>39</sup> In this study, we examined the surface modification of PLA using photo-activated  $\text{ClO}_2^*$  treatment to determine the effect of oxidation conditions on surface properties and to provide adhesion to metals or cellulose. In addition, we developed an oxidation method for powder samples.

## 2. Experimental

### 2.1. Materials

PLA (INGEO 2003D) was supplied by NatureWorks LLC. Sodium chlorite ( $\text{NaClO}_2$ ) and toluidine blue O (TBO) were obtained from Sigma-Aldrich. Hydrochloric acid ( $10 \text{ mol L}^{-1}$ ) was sourced from FUJIFILM Wako Pure Chemical Corporation. An aluminum plate was purchased from Nilaco and washed with ethanol prior to use.

<sup>a</sup> Graduate School of Pharmaceutical Sciences, Osaka University, Osaka, Japan.  
E-mail: asahara@phs.osaka-u.ac.jp

<sup>b</sup> Institute for Open and Transdisciplinary Research Initiatives, Osaka University,  
Osaka, Japan

<sup>c</sup> Department of Applied Chemistry, Graduate School of Engineering, Osaka  
University, Osaka, Japan. E-mail: uyama@chem.eng.osaka-u.ac.jp

† Electronic supplementary information (ESI) available. See DOI: <https://doi.org/10.1039/d4ma01275e>

‡ Present address: Department of Materials Science and Technology, Faculty of  
Advanced Engineering, Tokyo University of Science, Tokyo, Japan.



## 2.2. Preparation of PLA films

PLA was reprecipitated by adding a chloroform solution to methanol before use. The precipitate was then separated and dried overnight. The precipitated PLA was made into a film by thermal pressing for 10 min under 10 MPa at 170 °C. Powdered PLA with a diameter of approximately 1 mm was prepared by stirring a chloroform solution of PLA and gradually adding methanol.

## 2.3. Preparation of bacterial cellulose films

Bacterial cellulose (BC) sheets were prepared by thoroughly washing commercially available nata de coco and then dehydrating it by heat compression.

## 2.4. Modification of PLA films

The photo-activated  $\text{ClO}_2^\bullet$  gas treatment was carried out as follows. The PLA film surface was oxidized using the photo-activated  $\text{ClO}_2^\bullet$  gas generated from a 7-mL aqueous solution of  $\text{NaClO}_2$  (100 mg) and 10 M HCl aqueous solution (50  $\mu\text{L}$ ) under UV irradiation with an LED lamp ( $\lambda = 365 \text{ nm}$ , 20  $\text{mW cm}^{-2}$ ) in a set of Petri dishes covered with a glass plate (Fig. 1a). All the samples were washed with water and dried in a vacuum oven at 25 °C before oxidation. The PLA films were cut into an area of  $3 \times 1 \text{ cm}^2$ . The solution was placed in the inner small Petri dish, and the PLA film was placed next to the solution. The PLA films and aqueous solutions were irradiated with UV light. The oxidized samples were washed with water and dried in a vacuum oven at 25 °C prior to testing. The samples were cut to an appropriate size for subsequent tests.

The plasma treatment was carried out as follows. The PLA film was treated for 5 min using vacuum plasma equipment (Sakigake Semiconductor, YHS-R).

## 2.5. Characterization of the surface of the PLA films

The surface chemical composition analysis was performed as follows. The chemical compositions and functional groups were determined using attenuated total reflectance–Fourier transform infrared spectroscopy (FT/IR4700, JASCO) at 25 °C with a diamond window. All spectra were acquired at  $4 \text{ cm}^{-1}$

resolutions over 50 scans in the scan range of  $500\text{--}4000 \text{ cm}^{-1}$ . To confirm reproducibility, each measurement was performed on three samples. The surface elemental and chemical compositions of the PLA films were determined using X-ray photoelectron spectroscopy (XPS; Instrument: Kratos Ultra 2 with monochromatic Al  $K\alpha$  radiation, Shimadzu Corporation, Kyoto, Japan). The X-ray source was operated at 12 kV and 15 mA under standard conditions. Survey XPS spectra were obtained at binding energies of 0–1000 eV with an energy step of 1 eV. The high-resolution XPS spectra of C 1s were recorded with an energy step of 0.1 eV. Peak differentiation-imitating analysis of the high-resolution XPS spectra of C 1s was performed using the CasaXPS Version 2.3.15 software. The standard deviation of the data was obtained from two to five independent experiments.

The static water contact angles of the PLA films were determined using a Drop Master DM300 contact angle meter (Kyowa Interface Science, Saitama, Japan). A 1.0- $\mu\text{L}$  water droplet was placed on the surface of the PLA films, and the contact angle was determined immediately after the droplet was attached.

The TBO assay was performed as follows. The amount of carboxy groups on the PLA surfaces was determined by modifying the conditions based on the reported TBO assay.<sup>40</sup> PLA films were incubated in 2-mL TBO solution (1 mM NaOH, 0.1% TBO (Sigma-Aldrich, Germany)), (30 min, 25 °C, stirred at 1300 rpm). The films were washed with 1 mL of 1 mM aqueous NaOH to remove the excess TBO. This washing process was repeated until the supernatants were clear. Finally, TBO was desorbed by incubating the films in 10 mL of 20% sodium dodecyl sulfate (SDS) solution (30 min, 40 °C, stirred at 1300 rpm). The TBO absorption of the SDS supernatants was measured at 630 nm (spectrophotometer UV-1650PC, Shimadzu, Japan).

## 2.6. Adhesion of PLA to metal or cellulose

The adhesion of PLA to a metal plate or cellulose film was achieved using thermocompression bonding without any adhesives. The PLA film was cut into 2 mm  $\varnothing$  and was placed between two pieces of Al plate; thereafter, the thermocompression bonding was carried out at 185 °C for 10 min. Al/PLA/Al was loaded to failure at  $5 \text{ mm min}^{-1}$  in tensile mode, and the failure strain was measured. Data were recorded as the mean of three independent experiments with standard deviation. The PLA film was cut into  $4 \times 1 \text{ cm}^2$  and laminated onto cellulose film with a contact area of  $1 \text{ cm}^2$ , after which the thermocompression bonding was carried out at 160 °C under 10 MPa for 5 min. The PLA/cellulose was loaded to failure at  $5 \text{ mm min}^{-1}$  in tensile mode, and the failure strain was measured. Data were recorded as the mean of three independent experiments with standard deviation.

# 3. Results and discussion

## 3.1. Surface oxidation of the PLA film

Water contact angle measurements were conducted to investigate the hydrophilicity of the PLA surface after oxidation, using an oxidation setup (Fig. 1a). As shown in Fig. 1b, the



**Fig. 1** (a) Schematic image of the experimental method of PLA plate oxidation. (b) Images of water contact angles of the untreated, oxidized at 25 °C and oxidized at 70 °C PLA plates. (c) Relationship between reaction temperature and contact angle of the PLA plate.



hydrophobic surface of the untreated PLA with a contact angle of  $87^\circ$  was reduced to  $75^\circ$  by oxidation at  $25^\circ\text{C}$  for 10 min, indicating a slight improvement in hydrophilicity. A significant improvement in hydrophilicity was observed with the contact angle decreasing to  $44^\circ$  when the reaction was conducted by heating at  $70^\circ\text{C}$ . A study at different reaction temperatures was performed to investigate the effect of reaction temperature on hydrophilicity. As shown in Fig. 1c, the water contact angle decreased significantly at temperatures above around  $60^\circ\text{C}$ . This is likely ascribable to the fact that the reaction above the  $T_g$  of PLA ( $53^\circ\text{C}$ ) resulted in higher oxidation.

We attempted to characterize the functional groups using FTIR measurements; however, no significant changes were observed before and after oxidation. Although peaks derived from carbonyl groups were observed by IR measurement in a previous study for the oxidation of PP,<sup>31,32</sup> it was not detectable in PLA due to the overlap with the ester group peaks in the main chain (Fig. S1, ESI†). The surface elemental and chemical compositions of the PLA films treated under different oxidation conditions using photo-activated  $\text{ClO}_2^*$  gas were determined via XPS (Fig. S2, ESI†). The oxygen ratio on the surface of the untreated PLA film was 32.5%, whereas that of the oxidized PLAs increased as the oxidation time increased to 37.1% after 30 min (Table 1). On the other hand, the effect of heating was more significant, and the oxygen ratio increased to 39.5%, even after 10 min of oxidation. The increase in the oxygen ratio with the photo-activated  $\text{ClO}_2^*$  gas treatment is considered to be due to the conversion of methyl groups on PLA to carboxy groups, as reported previously. In fact, a decrease in the peak at 285 eV corresponding to C–C/C–H and an increase in the peak at 289 eV corresponding to O–C=O was observed in the oxidation sample (10 min,  $60^\circ\text{C}$ ) compared to the untreated sample in the chemical composition analysis based on the high-resolution C 1s spectra (Fig. S3, ESI†).

Based on the proportion of surface components determined by XPS analysis, a TBO absorption assay was used to quantify the number of carboxy groups on the PLA surface. The number of introduced carboxy groups per unit weight (defined as the oxidation degree) estimated by TBO staining of PLA samples ( $3 \times 0.5 \text{ cm}^2$ ,  $200 \mu\text{m}$  thickness) oxidized for 10 min at different temperatures is shown in Fig. 2b. The untreated PLA sample had a value of less than  $0.05 \mu\text{mol g}^{-1}$ , whereas the  $40^\circ\text{C}$  oxidized product exhibited an eightfold increase to  $0.4 \mu\text{mol g}^{-1}$ . Furthermore, the value was approximately  $2.0 \mu\text{mol g}^{-1}$  at  $60^\circ\text{C}$ . Thus, it was demonstrated that the potential for controlling the number

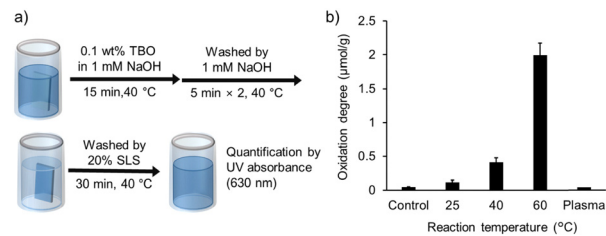


Fig. 2 (a) Schematic diagram of the TBO treatment for PLA plate. (b) Relationship between reaction temperature and oxidation degree (number of carboxy group) of PLA plates determined by the TBO treatment.

of carboxy groups on the PLA surface depends on the oxidation conditions. For comparison, the plasma-treated samples were examined to reveal that few carboxy groups were introduced.

Next, we attempted to apply the  $\text{ClO}_2^*$  photo-oxidation treatment to both the film and powder samples. For the oxidation of the powder samples, we used a device that rotated the sample to achieve homogeneous processing (Fig. 3a).  $\text{ClO}_2^*$  gas was independently generated and introduced via air pumping, and the powdered sample area was irradiated. This apparatus enabled the treatment of 10 g units at a time. The powder samples exhibited a higher oxidation degree at  $25^\circ\text{C}$  ( $1.3 \mu\text{mol g}^{-1}$ ) owing to their higher specific surface area per unit weight compared to the film samples (Fig. 3b). It is difficult to achieve large-volume treatment of powders using conventional plasma treatment.  $\text{ClO}_2^*$  photo-oxidation is applicable to various shapes and can be used as a surface modification method, complementary to conventional methods.

### 3.2. Adhesion of the surface-modified PLA films with aluminum plate and cellulose sheet

After confirming the introduction of carboxy groups as polar functional groups on the PLA surface via  $\text{ClO}_2^*$  gas photooxidation, adhesion tests were conducted with metals utilizing these functional groups. The adhesion strength was determined, and it was measured as a function of oxidation degree (Fig. 4). As shown in Fig. 4c, the adhesion strength of the untreated sample showed almost no adhesion to aluminum, whereas that of the oxidized sample increased gradually with an increasing oxidation degree (increase in the number of carboxy groups), reaching a maximum of approximately 20 MPa (regions I and II in Fig. 4c). In the peeled samples with an oxidation degree of less than  $0.1 \mu\text{mol g}^{-1}$ , the PLA resin was found only on one

Table 1 Summary of the atomic composition of the PLA surface under different reaction conditions

Reaction conditions		Atomic composition (%)		
Time (min)	Temperature ( $^\circ\text{C}$ )	Carbon	Oxygen	O/C ratio
0	25	67.5	32.5	0.48
5	25	64.6	34.4	0.53
10	25	63.9	35.3	0.55
30	25	60.7	37.1	0.61
10	60	60.2	39.5	0.66



Fig. 3 (a) Schematic image of experimental method for PLA powder oxidation. (b) Photographs of untreated and oxidized PLA powder with TBO staining and the values of oxidation degree estimated by TBO treatment.





Fig. 4 (a) Schematic images and pictures of before and after thermo-compression bonding of Al/PLA/Al. (b) Schematic illustration of the adhesion strength test. (c) Relationship between oxidation degree estimated by TBO treatment and adhesion strength.

side of the aluminum, indicating that interfacial peeling had occurred (photograph on the left in Fig. 4c). On the other hand, PLA resin remained on both sides of the aluminum plate after peeling in the sample that showed high adhesion strength, indicating that the peeling was caused by the substrate failure of PLA (photograph on the right in Fig. 4c). The adhesive strength decreased as the oxidation degree increased above  $0.3 \mu\text{mol g}^{-1}$  (region III in Fig. 4c). Although the introduction of polar functional groups on the PLA surface contributed to the improvement in its affinity with aluminum, excessive oxidation is considered to have decreased the strength of the PLA resin.

Next, the adhesion of the surface-modified PLA films to cellulose sheets was investigated. Cellulose sheets were prepared by heat compression of nata de coco. Untreated PLA and cellulose sheets showed no adhesion when thermocompression at  $80^\circ\text{C}$  was applied, although oxidized PLA and BC sheets

adhered strongly (Fig. 5). The adhesion strength between oxidized PLA ( $25^\circ\text{C}$ , 10 min) and BC was 0.9 MPa. It is clear that the surface oxidation of PLA improved its affinity for cellulose. The adhesive strength further increased to 1.1 MPa when oxidized PLA at  $65^\circ\text{C}$  for 10 min was used; however, the BC film was cleaved, and the exact strength could not be measured. These results indicate that the hydrogen bonds between the carboxylic acids on the PLA surface and the hydroxyl groups of cellulose are the driving forces for adhesion. Oxidized PLA, which can adhere not only to metallic materials but also to cellulose materials, contributes to the development of functionally degradable materials.

## 4. Conclusions

We demonstrated that PLA can be oxidized using the photo-activated  $\text{ClO}_2^*$  treatment and that the oxidation degree can be controlled depending on the oxidation conditions. The oxidized surface properties were strongly affected by the reaction temperature, with a significant decrease in the water contact angle and an increase in the number of oxygen functional groups introduced at temperatures above the  $T_g$  of PLA. The XPS analysis and TBO staining revealed that oxidation at higher temperatures introduced a larger number of oxygen functional groups, especially carboxy groups, onto the PLA surface. The photo-activated  $\text{ClO}_2^*$  treatment can be applied to the oxidation of powder samples, which are difficult to treat uniformly by conventional plasma treatment, and it can achieve efficient oxidation in a short time. The adhesion of oxidized PLA to dissimilar materials was also examined, and a change in the adhesion strength dependent on the oxidation degree was observed in adhesion with aluminum. This is considered to be a balance between the increase in the interaction with aluminum and the decrease in the PLA strength resulting from the increase in the number of functional groups. The results obtained in this study indicate that PLA, which lacks adhesive properties, enables adhesion to dissimilar materials, and is expected to contribute to expanding the range of applications of PLA and mitigating its environmental impact.

## Author contributions

H. A. designed this study and wrote the paper. H. A., W. W. and T. A. contributed to the experimental work. Y.-I. H. and T. I. contributed to the investigation. H. U. contributed to supervision and project administration.

## Data availability

The data supporting this article have been included as part of the ESI.†

## Conflicts of interest

There are no conflicts to declare.



Fig. 5 (a) Schematic images of before and after thermocompression bonding of PLA/cellulose. (b) Photograph of cellulose sheet using this study. (c) Photograph of a PLA and cellulose-adhered sample.



## Acknowledgements

This work was supported by the Japan Society for the Promotion of Science (JSPS) KAKENHI Grants (20K05606 & 23K18542, H. A.; 22K21348, Y.-I. H.; 23K26717, H. U.), the New Energy and Industrial Technology Development Organization (NEDO) grant (17101509-0, H. A.), and the Environmental Restoration and Conservation Agency (ERCA) grant (3RF-1802, T. A.). We also thank the experimental support of Ms Sawako Mukushita.

## Notes and references

- 1 S. Farah, D. G. Anderson and R. Langer, *Adv. Drug Delivery Rev.*, 2016, **107**, 367–392.
- 2 Y. Chen, L. M. Geever, J. A. Killion, J. G. Lyons, C. L. Higginbotham and D. M. Devine, *Polym.-Plast. Technol. Eng.*, 2016, **55**, 1057–1075.
- 3 N. Tripathi, M. Misra and A. K. Mohanty, *ACS Eng. Au*, 2021, **1**, 7–38.
- 4 R. Auras, B. Harte and S. Selke, *Macromol. Biosci.*, 2004, **4**, 835–864.
- 5 T. A. Swetha, A. Bora, K. Mohanrasu, P. Balaji, R. Raja, K. Ponnuchamy, G. Muthusamy and A. Arun, *Int. J. Biol. Macromol.*, 2023, **234**, 1–10.
- 6 D. S. Rajendran, S. Venkataraman, S. K. Jha, D. Chakrabarty and V. V. Kumar, *Food Sci. Biotechnol.*, 2024, **33**, 1759–1788.
- 7 S. M. Davachi and B. Kaffashi, *Polym.-Plast. Technol. Eng.*, 2015, **54**, 944–967.
- 8 A. K. Agrawal and R. Bhalla, *J. Macromol. Sci. C*, 2003, **43**, 479–503.
- 9 F. S. Fattahi, A. Khoddami and O. Avinc, in *Sustainability in the Textile and Apparel Industries. Sustainable Textiles: Production, Processing, Manufacturing & Chemistry*, ed. S. S. Muthu and M. A. Gardetti, Springer, Cham, Switzerland, 2020, pp. 173–194.
- 10 S. Teixeira, K. M. Eblagon, F. Miranda, R. M. F. Pereira and J. L. Figueiredo, *C*, 2021, **7**, 42.
- 11 P. J. Jandas, S. Mohanty and S. K. Nayak, *Ind. Eng. Chem. Res.*, 2013, **52**, 17714–17724.
- 12 J. R. Barbosa, P. H. O. Amorim, M. C. de O. Gonçalves, R. M. Dornellas, R. P. Pereira and F. S. Semaan, *Smart Innovation, Systems and Technologies*, Springer Singapore, 1st edn, 2020, vol. 152, pp. 425–435.
- 13 V. G. Muñoz, L. M. Muneta, R. Carrasco-Gallego, J. de Juanes Marquez and D. Hidalgo-Carvajal, *Appl. Sci.*, 2020, **10**, 8967.
- 14 C. H. Lee, F. N. B. M. Padzil, S. H. Lee, Z. M. A. Ainun and L. C. Abdullah, *Polymers*, 2021, **13**, 1407.
- 15 V. Cojocar, D. Frunzaverde, C.-O. Miclosina and G. Marginean, *Polymers*, 2022, **14**, 886.
- 16 M. R. Hasan, I. J. Davies, A. Pramanik, M. John and W. K. Biswas, *Sustainable Manuf. Serv. Econ.*, 2024, **3**, 100020.
- 17 P. S. Ferreira, S. M. Ribeiro, R. Pontes and J. Nunes, *Environ. Chem. Lett.*, 2024, **22**, 1831–1859.
- 18 R. M. Rasal, A. V. Janorkar and D. E. Hirt, *Prog. Polym. Sci.*, 2010, **35**, 338–356.
- 19 G. S. Mann, L. P. Singh, P. Kumar, S. Singh and C. Prakash, *J. Thermoplast. Compos. Mater.*, 2019, **34**, 977–1005.
- 20 C. Vergne, O. Buchheit, F. Eddoumy, E. Sorrenti, J. Di Martino and D. Ruch, *J. Eng. Mater. Technol.*, 2011, **133**, 030903.
- 21 A. Jorda-Vilaplana, V. Fombuena, D. Garcia-Garcia, M. D. Samper and L. Sanchez-Nacher, *Eur. Polym. J.*, 2014, **58**, 23–33.
- 22 A. Jordá-Vilaplana, L. Sánchez-Nácher, V. Fombuena, D. García-García and A. Carbonell-Verdú, *J. Appl. Polym. Sci.*, 2015, **132**, 42391.
- 23 M. Młotek, A. Gadomska-Gajadhur, A. Sobczak, A. Kruk, M. Perron and K. Krawczyk, *Appl. Sci.*, 2021, **11**, 1815.
- 24 G. D. Deepak, Atul and G. Anne, *Int. J. Multiphys.*, 2024, **18**, 01–16.
- 25 G.-H. Koo and J. Jang, *Fibers Polym.*, 2008, **9**, 674–678.
- 26 P. Bhati, A. Srivastava, R. Ahuja, P. Chauhan, P. Vashisth and N. Bhatnagar, *Polymers*, 2023, **15**, 1097.
- 27 H. Sun and S. Önnby, *Polym. Int.*, 2006, **55**, 1336–1340.
- 28 V. Korzhikov-Vlakh, E. Sinitsyna, K. Arkhipov, M. Levit, E. Korzhikova-Vlakh and T. Tennikova, *Surfaces*, 2024, **7**, 1008–1028.
- 29 F. J. Xu, X. C. Yang, C. Y. Li and W. T. Yang, *Macromolecules*, 2011, **44**, 2371–2377.
- 30 L. Yao, Y. Li, Y. Li, Y. Wang, L. Wang, D. Qiu and Y. Weng, *J. Appl. Polym. Sci.*, 2024, **141**, e55999.
- 31 K. Ohkubo, H. Asahara and T. Inoue, *Chem. Commun.*, 2019, **55**, 4723–4726.
- 32 Y. Jia, J. Chen, H. Asahara, T. Asoh and H. Uyama, *ACS Appl. Polym. Mater.*, 2019, **1**, 3452–3458.
- 33 K. Yamamoto, H. Asahara, M. Moriguchi and T. Inoue, *Polym. J.*, 2023, **55**, 599–605.
- 34 K. Yamamoto, H. Asahara, K. Harada, Y. Itabashi, K. Ohkubo and T. Inoue, *J. Mater. Chem. B*, 2023, **11**, 5101–5107.
- 35 Y. Jia, J. Chen, H. Asahara, Y.-I. Hsu, T. Asoh and H. Uyama, *Polymer*, 2020, **200**, 122592.
- 36 Y. Jia, H. Asahara, Y.-I. Hsu, T. Asoh and H. Uyama, *Appl. Surf. Sci.*, 2020, **530**, 147202.
- 37 Y. Jia, W. Wu, H. Asahara, Y.-I. Hsu, T. Asoh, H. TiangTan, K. Sudesh and H. Uyama, *Polym. Degrad. Stab.*, 2021, **191**, 109661.
- 38 Z. Cao, Y.-I. Hsu, A. Koizumi, H. Asahara, T. Asoh and H. Uyama, *Polym. J.*, 2021, **53**, 1231–1239.
- 39 B. Zhang, X. Wang, D. Wang, M. Guo, C. Ren, W. Han, H. Uyama and Q. Li, *ACS Appl. Bio. Mater.*, 2021, **4**, 2696–2703.
- 40 R. Stefan, M. Ruhland, C. Schmidt, C. Schr, K. Grossmann and B. Alexander, *Anal. Chem.*, 2011, **83**, 3379–3385.

